A Journal of the Gesellschaft Deutscher Chemiker

Angewandte International Edition GDCh Chemie

www.angewandte.org

Accepted Article

Title: CRISPR-Mediated Profiling of Viral RNA at Single Nucleotide Resolution

Authors: Duo Chen, Wanting Huang, Yun Zhang, Bo Chen, Jie Tan, Yanbing Yang, and Quan Yuan

To be cited as: *Angew. Chem. Int. Ed.* **2023**, e202304298

Link to VoR: https://doi.org/10.1002/anie.202304298

WILEY VCH

10.1002/anie.202304298

WILEY-VCH

RESEARCH ARTICLE

CRISPR-Mediated Profiling of Viral RNA at Single-Nucleotide Resolution

Duo Chen[a],⊥, Wanting Huang[a],⊥, Yun Zhang[a],⊥, Bo Chen[a], Jie Tan[b], Quan Yuan*[a,b], Yanbing Yang*[a]

⊥These authors contributed equally to this work.

[a] D. Chen, W. Huang, Y. Zhang, B. Chen, Prof. Q. Yuan, and Prof. Y. Yang
College of Chemistry and Molecular Sciences, Key Laboratory of Biomedical Polymers of Ministry of Education, Institute of Molecular Medicine, Renmin Hospital of Wuhan University, School of Microelectronics
Wuhan University, Wuhan 430072, P. R. China
E-mail: yangyanbing@whu.edu.cn.
E-mail: yuanquan@whu.edu.cn.

[b] J. Tan, and Prof. Q. Yuan
Molecular Science and Biomedicine Laboratory (MBL), State Key Laboratory of Chemo/Biosensing and Chemometrics, College of Chemistry and Chemical Engineering
Hunan University, Changsha 410082, P. R. China

Supporting information for this article is given via a link at the end of the document.

Abstract: Mass pathogen screening is critical to preventing the outbreaks and spread of infectious diseases. The large-scale epidemic of COVID-19 and the rapid mutation of the severe acute respiratory syndrome coronavirus 2 (SARS-CoV-2) virus have put forward new requirements for virus detection and identification techniques. Here, we report a CRISPR-based Amplification-free Viral RNA Electrical Detection platform (CAVRED) for the rapid detection and identification of SARS-CoV-2 variants. A series of CRISPR RNA assays were designed to amplify the CRISPR-Cas system's ability to discriminate between mutant and wild RNA genomes with a single-nucleotide difference. The identified viral RNA information was converted into readable electrical signals through field-effect transistor biosensors for the achievement of highly sensitive detection of single-base mutations. CAVRED can detect the SARS-CoV-2 virus genome as low as 1 cp/μL within 20 mins without amplification, and this value is comparable to the detection limit of real-time quantitative polymerase chain reaction. Based on the excellent RNA mutation detection ability, an 8-in-1 CAVRED array was constructed and realized the rapid identification of 40 simulated throat swab samples of SARS-CoV-2 variants with a 95.0% accuracy. The advantages of accuracy, sensitivity, and fast speed of CAVRED promise its application in rapid and large-scale epidemic screening.

Introduction

The large-scale outbreak of COVID-19 and the rapid mutation of SARS-CoV-2 virus have brought unprecedented challenges to the prevention and control of the epidemic.[1] The emergence of new variants has increased the uncertainty of virus transmission, pathogenicity, and vaccine effectiveness, posing a great threat to public health security.[2] The Omicron BA.5 variant, which is currently dominant worldwide, is more infectious than the ancestral lineage and has no specific therapeutic drugs to date.[3] The latest World Health Organization (WHO) report identifies increasing diversity in the lineage of descendants of SARS-CoV-2 Omicron variant.[4] Among these descendants, some severe variants, such as BF.7 and BQ.1, demonstrated substantial neutralization escape ability.[5] The development of effective methods for patient-specific detection and identification of SARS-CoV-2 and its variants is helpful in accurately assessing the infectivity and lethality risk of the virus, which is essential for providing specific treatment, curbing the spread of the epidemic, and guiding the development of vaccines.[6] An ideal method for the patient-specific detection of viral RNA should be fast and sensitive, independent of large equipment, and capable of identifying multiple variants.[7] Currently, the detection and identification of SARS-CoV-2 variants are mainly achieved by reverse transcriptase polymerase chain reaction (RT-PCR) and whole genome sequencing (WGS).[8] RT-PCR relies on large equipment and cannot identify multiple variants simultaneously. WGS requires a complex operation, long operation time, and tedious sample handling. Detection assays based on isothermal amplification strategies, such as loop-mediated isothermal amplification,[9a,8b] recombinase polymerase amplification,[9c] strand displacement amplification,[9c] and rolling circle amplification,[9d,9e] reduce the need for temperature control instruments and shorten the detection time. However, the above methods usually require tedious amplification procedures, increasing the complexity of the operation, and their potential has so far not been sufficiently developed for detecting multiple RNA mutations of SARS-CoV-2 variants. The development of a convenient, rapid, and highly sensitive detection method for SARS-CoV-2 and its variants identification is essential for epidemiological surveillance.

CRISPR diagnostic (CRISPR-Dx) technologies can specifically recognize the target sequences through CRISPR RNA (crRNA), and output detection signals by activating CRISPR-associated proteins (Cas) to cleave DNA or RNA reporters.[10] With the advantages of high specificity, simple operation, and portability, CRISPR-Dx has been successfully utilized in the development of multifunctional nucleic acid detection platforms.[11] Commercial detection platforms based on CRISPR-Dx, such as specific high-sensitivity enzymatic reporter

10.1002/anie.202304298

unlocking (SHERLOCK) and DNA endonuclease targeted CRISPR trans reporter (DETECTR), have been successfully developed for the detection of SARS-CoV-2.[11a,11b] Advances in amplification-free CRISPR-Dx technologies, including the superactive LwaCas13a effector,[12a] CRISPR-mobile phone microscope,[12b] gFET-based LwaCas13a system,[12c] and E-CRISPR,[12d] effectively avoid tedious laboratory settings and shortens the assay time, thus promoting the application of CRISPR-Dx in pathogen screening and infectious disease diagnostics.[12e,12f] However, CRISPR-Dx still faces challenges in the application of SARS-CoV-2 variants identification. Generally, Cas proteins, especially Cas9 and Cas13a, tolerate single-base mismatches between crRNA and target sequences and have limited discrimination in identifying single-base mutations in SARS-CoV-2 variant genomes.[13] The exploration of multiplexed, highly sensitive, amplification-free CRISPR-Dx technologies for the rapid detection and identification of SARS-CoV-2 and its variants at single-nucleotide resolution is highly required while remaining a great challenge.

Herein, we developed a CRISPR-based Amplification-free Viral RNA Electrical Detection platform (CAVRED) to achieve efficient detection and identification of SARS-CoV-2 and its variants. CAVRED could recognize viral RNA by crRNA complementation and output electrical signals through the field-effect transistor (FET) arrays. The developed crRNA assays with modified synthetic mismatches in the spacer sequences allow the identification of RNA mutations for single-base substitutions and multiple-base deletions in the SARS-CoV-2 genome. CAVRED utilizes the intrinsic signal amplification capability of FET to amplify the recognition event of single-base mutations to achieve amplification-free, highly sensitive detection of viral RNA within 20 mins. CAVRED realizes the detection of SARS-CoV-2 RNA genomes as low as 1 cp/μL, which is comparable to the detection limit of RT-PCR.[14] For 40 simulated throat swab samples, CAVRED is capable of accurately detecting and identifying SARS-CoV-2 variants with a 95.0% accuracy. Our design provides an efficient approach to the development of portable and rapid technologies for the detection and screening of epidemic viruses.

Results and Discussion

Scheme 1 shows the working principle of the CAVRED for the detection and identification of SARS-CoV-2 variants. CAVRED can be divided into two parts, including a viral RNA recognition unit and a signal output unit. The RNA recognition unit consists of Cas13a and the corresponding crRNA. The signal output unit consists of FET arrays modified with RNA reporters that could transduce the information of viral RNA into a readable electrical signal. The synthetic mismatch in crRNA was optimized to control the trans-cleavage activity of Cas13a protein, thereby achieving the specifically wild type or mutated viral RNA recognition. As shown in Scheme 1, Cas13a exhibits higher cleavage activity when the mutant-specific crRNA binds to the mutated RNA sequences with a higher matching degree. In comparison, when the mutant-specific crRNA binds to the wild-type RNA sequences, Cas13a is difficult to be triggered due to the poor sequence matching, resulting in a weak cleavage activity. Based on this principle, Cas13a exhibits better trans-cleavage of RNA reporters only in the presence of mutated viral RNA. The cleavage of the RNA reporters by Cas13a is amplified by a FET signal output unit and converted into a readable electrical signal. By analyzing the electrical signals, CAVRED can distinguish mutated viral RNA from the wild type, which in turn enables the identification of SARS-CoV-2 variants, including Alpha, Beta, Gamma, Delta, and Omicron.

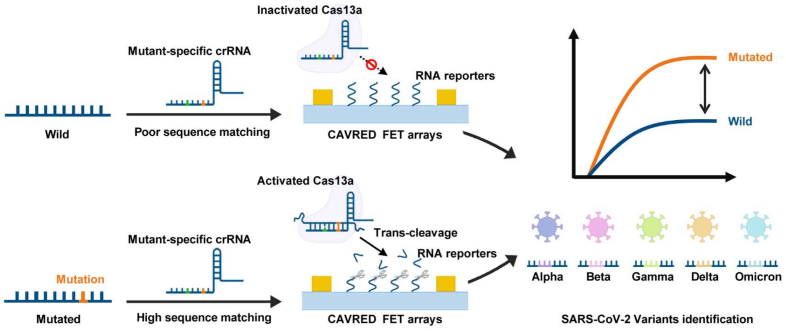

Scheme 1. The working principle of CAVRED in the detection and identification of SARS-CoV-2 and its variants. The trans-cleavage of Cas13a was alternatively activated by mutant-specific crRNA, which has a different sequence matching between the wild and the mutated viral RNA. The output signal was further amplified by the CAVRED FET array to achieve RNA profiling at single-nucleotide resolution, which in turn enables the identification of SARS-CoV-2 variants, including Alpha, Beta, Gamma, Delta, and Omicron.

Design of CAVRED-crRNA for the detection of SARS-CoV-2 and its variants.

There are two representative forms of mutation in the genomes of SARS-CoV-2 variants. One is single-base substitutions at a specific amino acid site. For example, the SARS-CoV-2 variants contain three single-base substitutions at the 417 amino acid position of S gene, including Wild 417 (present in the wild type), K417N (present in Beta and Omicron variants), and K417T (present in Gamma variant).[11d] The other is a multiple-base deletion at consecutive amino acid sites, such as the IHV68-70I mutation present in Alpha and Omicron variants.[7a]

10.1002/anie.202304298

RESEARCH ARTICLE

In order to sensitively identify the RNA mutations in SARS-CoV-2 variants, we designed sets of crRNAs that exhibit differential activities on the wild-type RNA genome with respect to the mutated RNA genome. Previous studies have highlighted the importance of positions 3, 5, and 24 to Cas13a activity on single nucleotide polymorphisms (SNPs) identification,[10a,11b] thus we manually designed 6 crRNAs based on the above-selected sites to detect the 417 mutation. The specificity and activity of Cas13a were quantified by the fluorescence intensity, and the discrimination factor was defined as the ratio of fluorescence intensity between K417N and Wild 417 RNA sequences (Figure 1a, Figure S1-S3). Compared with no synthetic mismatch, the introduction of single synthetic mismatches into crRNA targeting K417N mutation resulted in a 2~3 folds increase in the discrimination factor (Figure S1). Meanwhile, in the presence of two synthetic mismatches, Cas13a exhibits lower activity and requires a longer time to be triggered. The discriminating factor reaches the maximum of 7.5 when the target mutation was set at position 3 and the synthetic mismatch was located at position 5, and the crRNA was selected for the identification of K417N genome (Figure S2 and S3). The turnover rates (k_{cat}) of Cas13a toward K417N and Wild 417 RNA sequences are calculated as 3.2 s^{-1} and 0.5 s^{-1} respectively, indicating that the designed crRNA could effectively discriminate wild-type and mutated RNA at single-nucleotide resolution (Figure S4). Similarly, we designed crRNA targeting Wild 417 and K417T genomes and demonstrated that our designed 417 assays could identify three genotypes with high accuracy (Figure 1a, 1c).

Unlike the 417 mutations with single-base substitutions, the 67-70 amino acid site of SARS-CoV-2 S gene contains not only a single-base substitution of A67V (present in the Omicron variant) but also IHV68-70I (present in the Alpha variant) with a six-base deletion. Consequently, both RNA mutations need to be considered in the design of the 67-70 crRNA assays. When the target mutation was placed at position 3 or 5, the crRNA could only detect the A67V mutation but ignore the mutation of IHV68-70I. In contrast, when the target mutation was placed at position 24 and the synthetic mismatch was introduced at position 3, the obtained crRNA could identify the presence of both A67V and IHV68-70I mutations. As shown in Figures 1b and 1c, the designed 67-70 crRNA assays exhibit high accuracy in the identification of three genotypes (Wild 67-70, IHV68-70I, and A67V + IHV68-70I), respectively.

After demonstrating that the designed 417 and 67-70 crRNA assays can effectively identify short synthetic RNA sequences,

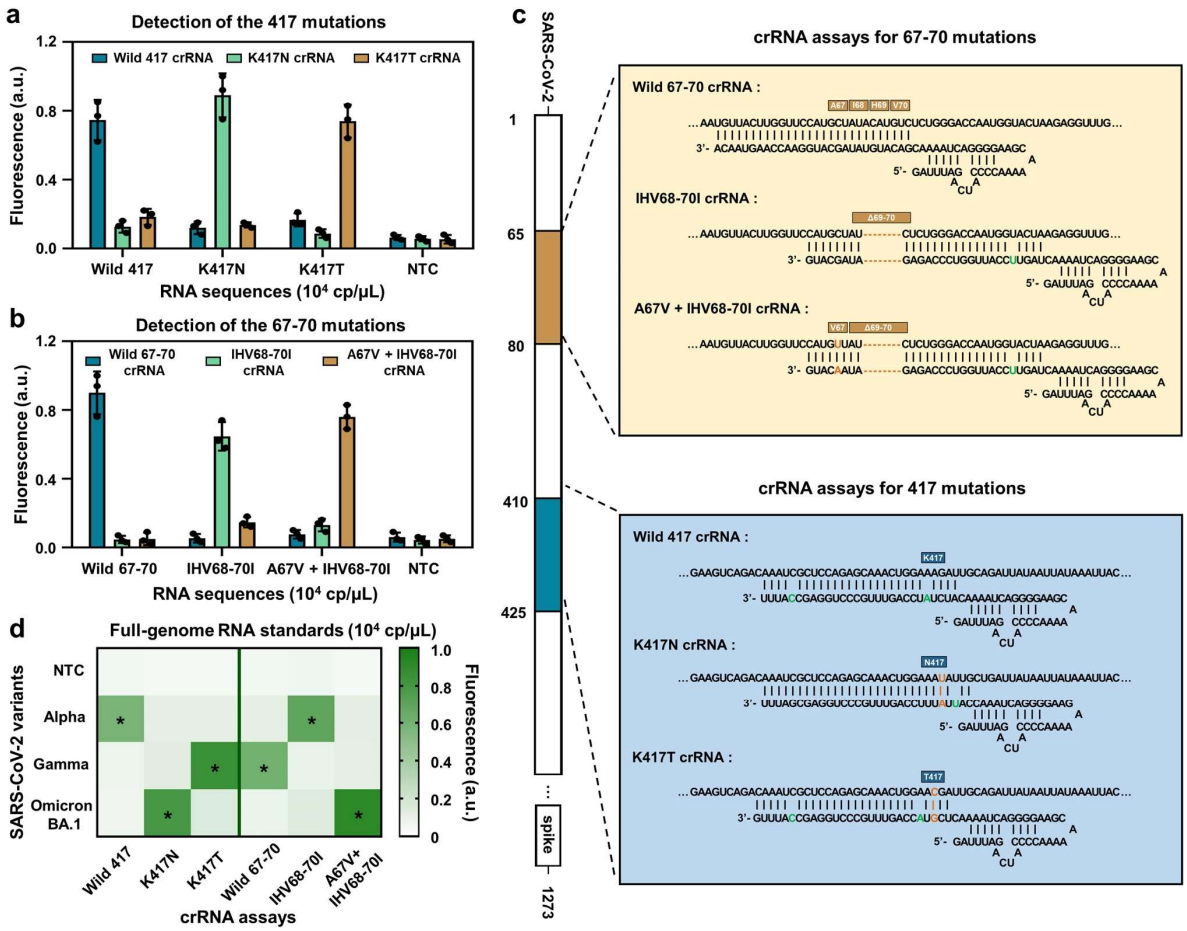

Figure 1. Design of CAVRED crRNA assays for the detection of SARS-CoV-2 variants. (a) Fluorescence intensity of 417 crRNA assays on RNA targets of 417 mutations. Target RNA concentration: 10^4 cp/μL; NTC: No target control. (b) Fluorescence intensity of 67-70 crRNA assays on RNA targets of 67-70 mutations. Target RNA concentration: 10^4 cp/μL. (c) Schematic of the mutations on SARS-CoV-2 S gene and the designed CAVRED-crRNA assays. Genomic sites with mutations in the SARS-CoV-2 variants are highlighted in orange. Synthetic mismatches introduced in crRNA are highlighted in green. (d) Identification of SARS-CoV-2 variants using 417 and 67-70 crRNA assays on full-genome RNA standards. Target RNA concentration: 10^4 cp/μL. Data in (a), (b), and (d) were expressed as mean ± s.d. for 3 technical replicates.

10.1002/anie.202304298

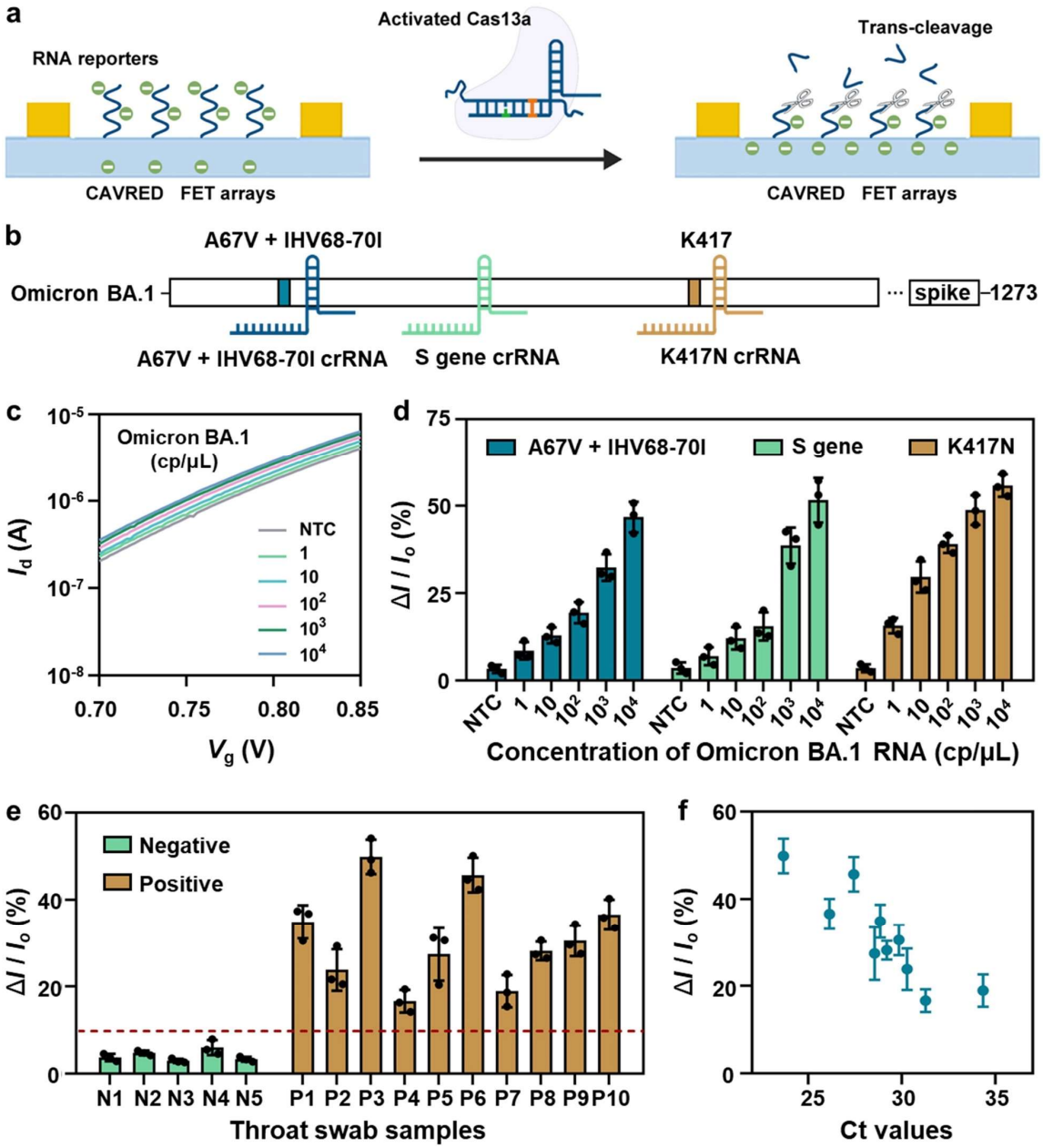

Figure 2. Evaluation of CAVRED performance on the detection of SARS-CoV-2 genome. (a) Working principle of FET biosensors in CAVRED for the amplification-free detection of viral RNA. (b) Schematic of the mutations on S gene of the Omicron variant and the selected crRNA assays. (c) I_d-V_g curves of the CAVRED with K417N crRNA in response to different concentrations of Omicron RNA genomes. (d) Current responses of the CAVRED in response to different concentrations of Omicron RNA genomes with A67V + IHV68-70I crRNA (blue), S gene crRNA (green), and K417N crRNA (brown). (e) Current responses of the CAVRED toward negative (N, green) and positive (P, brown) SARS-CoV-2 samples. (f) Current responses of the CAVRED plotted against RT-PCR Ct values toward simulated positive SARS-CoV-2 samples. Data in (d), (e), and (f) were expressed as mean ± s.d. for 3 technical replicates.

we then investigated their performance on full-genome RNA standards. As shown in Figure 1d, for the three different variants, 417 and 67-70 crRNA assays both correctly identified the presence or absence of the mutant gene. IHV68-70I crRNA and K417T crRNA show the highest fluorescence intensity in the detection of Alpha and Gamma variants, indicating that IHV68-70I and K417T RNA mutations are present in Alpha and Gamma variants, respectively. Similarly, we identified the presence of K417N, A67V + IHV68-70I RNA mutations in the Omicron variant (Figure S5, S6). These results are consistent with the RNA mutations of Alpha, Gamma, and Omicron variants confirmed by the previous report.[15] The above results indicate that our designed crRNA can effectively identify the mutations in SARS-CoV-2 genome.

Rapid detection of SARS-CoV-2 RNA by CAVRED.

In order to convert the SARS-CoV-2 mutations recognized by Cas13a into readable electrical signals, RNA reporters were modified at the interface of amino groups-treated indium gallium zinc oxide (IGZO) FET with the assistance of 4-(N-Maleimidomethyl)cyclohexane-1-carboxylic acid 3-sulfo-N-hydroxysuccinimide ester crosslinking reagent (Figure S7). In the presence of target RNA genome, Cas13a is activated to cleave

the negatively charged reporters, causing a change in the charge density on the surface of the FET, which in turn leads to a change in the response current (I_d) (Figure 2a). The presence of phosphate skeleton (1240 cm^{-1}) absorption peak in attenuated total reflection Fourier transforms infrared spectroscopy (ATR-FTIR) and the characteristic peaks of C 1s (286.6 eV), N 1s (399.9 eV), S 2p (162.4 eV), and P 2p (132.5 eV) in X-ray photoelectron spectroscopy (XPS) suggest that the RNA reporters were successfully modified on the FET interface (Figure S8 and S9).[16] Atomic force microscopy (AFM) characterization shows the formation of a uniform functional layer on the surface of FET with an average height of ~4.0 nm, which is consistent with the theoretical vertical height of the RNA reporters (Figure S10). Additionally, the modified FET exhibits stable current-time response in the PBS solution, indicating that RNA reporters were firmly immobilized at the FET interface (Figures S11 and S12). Subsequently, FAM fluorophores were introduced into the RNA reporters, and the changes in fluorescence intensity were observed before and after the trans-cleavage of Cas13a. As shown in Figure S13, the fluorescence intensity on the FET surface was significantly reduced after the trans-cleavage reaction, proving that Cas13a could maintain nuclease activity on the FET interface.

The SARS-CoV-2 variants RNA detection performance of the CAVRED was assessed by Omicron full-genome RNA standard. A67V + IHV68-70I and K417N are two key mutations in the Omicron BA.1 genome, which were regarded as the identification basis of the Omicron BA.1 variant.[10a] In addition, a CDC-certified S gene amplicon was also selected for the detection of Omicron genome (Figure 2b). According to the above-mentioned three gene sequences, we designed three different crRNAs, including A67V + IHV68-70I crRNA, K417N crRNA (mentioned in Figure 1a), and S gene crRNA. The reaction conditions of CRISPR system play a vital role in the detection performance of CAVRED. The optimized Cas13a concentration (50 nM), Mg^{2+} concentration (10 mM), Cas13a incubation time (20 min), and length of RNA reporters (15 nt) were chosen in the following measurements to achieve the optimal biosensing sensitivity (Figure S14). As shown in Figure 2c, I_d shows a significant increase upon the introduction of the target genome. The increased I_d is due to the electron transfer from the RNA phosphate backbones to the FET being reduced when the negatively charged RNA reporters were cleaved off from the FET upon the recognition of crRNA. The current response ($100 \times \Delta I/I_o$) is defined as the percentage change in I_d before and after target recognition (ΔI) compared with the initial current (I_o) of the FET. As shown in Figure 2d, CAVRED with K417N crRNA produced a significant current response of 11.6% towards the Omicron BA.1 genome with a concentration as low as 1 cp/μL, which is obviously higher than the current response of no target control (NTC, 3.7%). As the increase of the concentration of the target genome, more RNA reporters were cleaved off from the FET interface, and the current response increases gradually. Similarly, CAVRED exhibits a similar response performance to K417N in detecting the A67V + IHV68-70I mutation and the S gene sequences (Figure S15). It is worth noting that CAVRED can detect the viral RNA genome at a low concentration of 1 cp/μL without the need for an amplification process, which is comparable to the detection limit of RT-PCR. [14] The high sensitivity of CAVRED is attributed to the multi-turnover trans-cleavage of Cas13a as well as the signal amplification ability of the FET.[12c,17] The above results demonstrate that our designed CAVRED could achieve highly sensitive detection of the full-genome RNA of SARS-CoV-2 variants.

To evaluate the practical application potential of CAVRED, a full-genome RNA standard of the Omicron variant (concentration ranging from 1 to 10^4 cp/μL) was added to the negative throat swab samples to simulate the positive throat swab samples. CAVRED also demonstrated promising performance in simulated throat swab samples, identifying viral RNA at concentrations as low as 1cp/uL (Figure S16). For a step further, we recorded the current responses of 10 positive samples and 5 negative samples by CAVRED. As shown in Figure 2e, the current response of the positive samples is significantly higher (more than 14.2%) than that of negative samples (less than 7.9%), indicating that the CAVRED could distinguish between the negative samples and the positive samples. The Ct values of simulated positive samples were also measured with RT-PCR (Table S2). Figure 2f presents the plot of RT-PCR Ct values *versus* CAVRED current responses in the detection of the simulated samples. It can be observed that CAVRED produces a large current response for samples with a low Ct value, and a low current response for samples with a larger Ct value, indicating a semi-quantitative concentration correlation between the two detection methods. These results indicate that the CAVRED exhibits the ability to be ultrasensitive and accurate detection of the SARS-CoV-2 genome in simulated throat swab samples.

Identification of RNA mutations with CAVRED.

Alpha, Beta, Gamma, Delta, and Omicron variants are recommended as the most critical SARS-CoV-2 variants by the World Health Organization (WHO).[18] Consequently, nine critical mutations in the genome of these variants were selected as the detection targets of CAVRED, including A67V, IHV68-70I, EFR156-158G, R346T, K417N, K417T, N460K, E484K, and D614G (Figure 3a). In addition to A67V + IHV68-70I and K417N mentioned above for the identification of Omicron variants, D614G can distinguish between wild type and mutated SARS-CoV-2 genome. IHV68-70I and EFR156-158G are the representative mutations of Alpha and Delta variants, respectively. The Beta and Gamma variants can be distinguished by the K417T and K417N RNA mutations. In addition, the R346T mutation was chosen in view of the recent emergence of highly infectious Omicron BF.7 variant, and the N460K was selected for the identification of Omicron BQ.1 variant. The relationship between each RNA mutation and SARS-CoV-2 variants is shown in Figure 3b.

The CAVRED in profiling RNA mutations in the genome of the above-mentioned SARS-CoV-2 variants was then evaluated. A set of crRNAs targeting each RNA mutation was designed according to the principle in Figure 1c, and the current responses of CAVRED toward wild-type RNA and mutated RNA were measured (Figure S15). Figure 3c shows that the current response of CAVRED towards mutated RNA is more than 3.9 times higher than that for the wild-type RNA when the same concentration of RNA sequences was exploited. These results indicate that CAVRED shows the ability to identify nine representative RNA mutations mentioned above. Subsequently, the RNA mutations in the full-genome RNA standard were detected by CAVRED (Figure S16 and S17). As shown in Figure 3d, the current response of CAVRED for the IHV68-70I target mutation increases gradually with the increase of the

10.1002/anie.202304298

concentration of the Alpha genome, while the current response remains basically unchanged for the wild-type RNA. Specifically, CAVRED generates a 17.5% current response to 1 cp/μL of the Alpha genome, whereas the current response value was only 11.8% for the wild-type genome at concentrations up to 1000 cp/μL. Similarly, CAVRED for the K417T target mutation produces a 13.1% current response to 1 cp/μL of Gamma genome, but only 7.2% to 1000 cp/μL of wild-type RNA (Figure 3e). These results demonstrate that CAVRED can effectively profile RNA mutations in the SARS-CoV-2 genome.

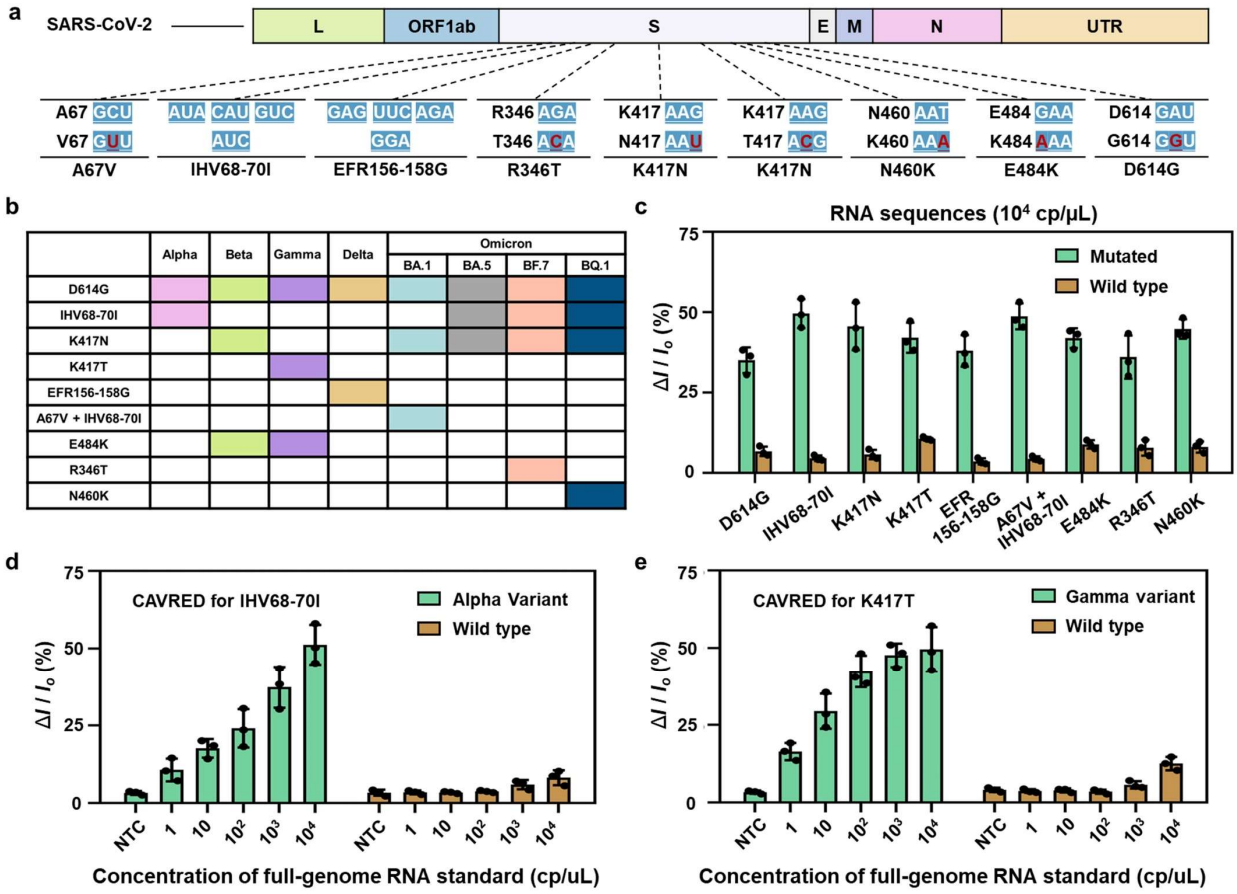

Figure 3. Identification of SARS-CoV-2 RNA mutations with CAVRED. (a) Schematic of the representative RNA mutations in the SARS-CoV-2 variant genome. (b) Correspondence between critical RNA mutations and SARS-CoV-2 variants including Alpha, Beta, Gamma, Delta, Omicron, and Omicron BF.7. (c) Current responses of CAVRED in response to the mutated (green) and the wild-type (brown) RNA sequences. Target RNA concentrations: 10^4 cp/μL. (d) Current responses of CAVRED with IHV68-70I crRNA in response to different concentrations of Alpha (green) and wild-type (brown) RNA genomes. (e) Current responses of CAVRED with K417T crRNA in response to different concentrations of Gamma (green) and wild-type (brown) RNA genomes. Data in (c), (d), and (e) were expressed as mean ± s.d. for 3 technical replicates.

Multiplexed detection of SARS-CoV-2 variants by CAVRED arrays.

Having validated the ability of CAVRED in profiling nine critical RNA mutations associated with Alpha, Beta, Gamma, Delta, and Omicron variants, an 8-in-1 CAVRED array was constructed to simultaneously identify the above five SARS-CoV-2 variants. As shown in Figure 4a, the CAVRED array consists of eight FET biosensing channels and two Ag/AgCl reference electrodes. Channels 2-8 could realize the simultaneous detection of D614G, IHV68-70I, K417N, K417T, EFR156-158G, A67V + IHV68-70I, and E484K RNA mutations. Channel 1 for the detection of S gene was introduced as a reference. The selected S gene sequences are present in all SARS-CoV-2 genomes and could be used to evaluate the validity of the measurement results. The 8 FET channels are separated by the polydimethylsiloxane solution cell to avoid interference between each channel. The current response of CAVRED towards the wild type and five variants (Alpha, Beta, Gamma, Delta, and Omicron BA.1) of SARS-CoV-2 full-genome RNA standards was evaluated (Figure 4b). For the Alpha variant, channels 1, 2, and 3 (corresponding to D614G, IHV68-70I, and S gene, respectively) of the CAVRED array exhibit higher current responses, indicating that CAVRED could identify the D614G and IHV68-70I mutations in Alpha RNA genome (Figure S18). For the Beta variant, channels 1, 2, 4, and 8 (corresponding to D614G, K417N, E484K, and S gene, respectively) exhibit higher current responses, indicating that the D614G and K417N mutations are correctly profiled (Figure S19). The same results were observed for the wild type and other mutated (Gamma, Delta, and Omicron BA.1) SARS-CoV-2 full-genome RNA standards. Figure 4c correlates the identified RNA mutations and the SARS-CoV-2 variants measured by the CAVRED array, and the results are consistent with the gene profiles of SARS-CoV-2 variants reported in the literature.[15,19] These results indicate that CAVRED can realize the simultaneous

10.1002/anie.202304298

detection of multiple RNA mutations in the genome of SARS-CoV-2, thus achieving effective identification of SARS-CoV-2 variants.

CAVRED array was then utilized to identify SARS-CoV-2 variants in practical scenarios. We first challenged CAVRED's ability to identify mutated RNA in throat swab samples. In a negative throat swab sample containing 10^4 cp/uL of the wild-type RNA genome, we added 1 cp/uL of RNA genomes from different SARS-CoV-2 variants and measured the current responses of each channel before and after the addition. As shown in Figure S22, current responses of CAVRED to the SARS-CoV-2 genome were significantly increased in the presence of relevant RNA mutations, indicating that CAVRED assay can identify the presence of mutant RNA genomes at concentrations as low as 1 cp/uL. For a step further, double-blind experiments were performed with 40 simulated positive samples obtained by adding SARS-CoV-2 genomes of different variants to the negative throat swab samples (Table S3). Figure 4d shows the detection results of 40 simulated samples by the 8-in-1 CAVRED array. According to the current responses of different channels in the CAVRED array, the RNA mutations present in the simulated samples were determined to identify the variant type according to the gene profile in Figure 4c. For example, for simulated sample 1, the CAVRED array detected the presence of D614G, K417N, and A67V + IHV68-70I mutations, thus sample 1 was determined to be Omicron BA.1 variant (Figure S23). The overall statistical results indicate that CAVRED made correct judgments in 38 out of 40 simulated samples, with an accuracy of 95.0%. S gene was not detected in samples 17 and 31, and the results were considered invalid (Figure S24 and S25). The reason may be due to that the low concentration of added viral RNA genome results in a negligible current response of the CAVRED array. It is worth mentioning that the detection time of the CAVRED array for simulated throat swab samples is no more than 20 mins in total, including the time from sampling to the output of test results. Overall, these results highlight that CAVRED can achieve rapid and accurate identification of SARS-CoV-2 variants, and is adapted to the requirements of large-scale, rapid, and point-of-care SARS-CoV-2 screening and variants identification in practical applications.

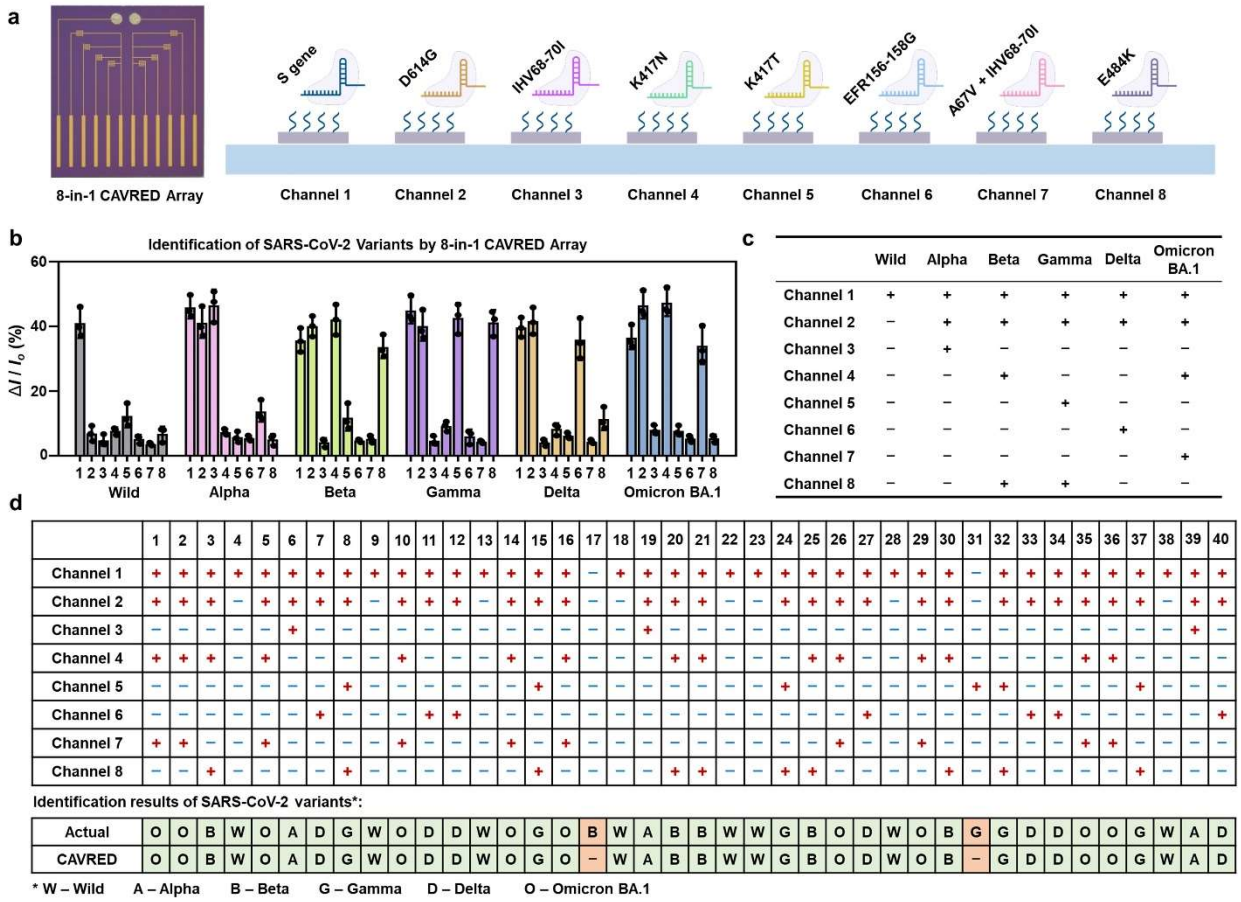

Figure 4. Identification of multiple SARS-CoV-2 variants by CAVRED array. (a) Photograph and schematic of 8-in-1 CAVRED array, in which 8 channels are targeted for D614G, IHV68-70I, K417N, K417T, EFR156-168G, A67V + IHV68-70I, and E484K RNA mutations and S gene of SARS-CoV-2 genomes. (b) Current responses of 8-in-1 CAVRED array toward RNA genomes of different SARS-CoV-2 variants including the wild type, Alpha, Beta, Gamma, Delta, and Omicron. (c) Correspondence between the detection results of 8-in-1 CAVRED arrays and the SARS-CoV-2 variants. (d) Identification results of SARS-CoV-2 and its variants for 40 simulated positive throat swab samples with 8-in-1 CAVRED arrays. The green shadow indicates the correct identification results while the red shadow indicates the incorrect identification results. Data in (b) were expressed as mean ± s.d. for 3 technical replicates.

Conclusion

In conclusion, we developed a CAVRED to realize highly sensitive detection of SARS-CoV-2 virus RNA and accurate identification of SARS-CoV-2 variants. For wild-type and mutated SARS-CoV-2 RNA, we designed sets of crRNAs to specifically recognize the target sequences by optimizing the location of synthetic mismatches. The designed crRNA assays exhibit

differential activities on the mutant RNA genome with respect to the wild type. Based on the designed CAVRED, we achieve the detection of full-genome RNA of Omicron. CAVRED can detect viral RNA as low as 1 cp/μL within 20 mins and demonstrate detection performance comparable to that of RT-PCR in simulated sample tests. CAVRED was verified to be capable of profiling 9 critical RNA mutations in the S gene of SARS-CoV-2. An 8-in-1 CAVRED array was constructed to achieve the simultaneous detection of multiple RNA mutations in the full genome of SARS-CoV-2, thus realizing the effective identification of multiple SARS-CoV-2 variants. In the identification test on 40 simulated throat swab samples of different SARS-CoV-2 variants, CAVRED exhibits a discrimination accuracy of up to 95.0%. Overall, the remarkable performance of CAVRED in the detection and identification of SARS-CoV-2 variants not only suggests a pathway to achieve rapid point-of-care detection and scalable epidemic screening but also provides a strategy to design an efficient detection platform for RNA-relevant diseases.

Acknowledgments

The National Key R&D Program of China (2017YFA0208000, 2021YFA1202400), the National Natural Science Foundation of China (21925401), the Fundamental Research Funds for the Central Universities (2042022rc0004), and the Tencent Foundation are acknowledged for research funding. We thank the Core Facility of Wuhan University for SEM, ATR-FTIR, and XPS analysis. The study was approved by the Ethics Committee of Renmin Hospital of Wuhan University (WDRY2022-K257).

Keywords: CRISPR Diagnostic, RNA Profiling, Single Nucleotide Polymorphism, Field Effect Transistor, SARS-CoV-2 Variants

[1] a) W. F. Garcia-Beltran, E. C. Lam, K. St Denis, A. D. Nitido, Z. H. Garcia, B. M. Hauser, J. Feldman, M. N. Pavlovic, D. J. Gregory, M. C. Poznansky, A. Sigal, A. G. Schmidt, A. J. Iafrate, V. Naranbhai, A. B. Balazs, *Cell* **2021**, *184*, 2372–2383 e2379; b) A. Fontanet, B. Autran, B. Lina, M. P. Kieny, S. S. A. Karim, D. Sridhar, *Lancet* **2021**, *397*, 952–954; c) D. M. Altmann, R. J. Boyton, R. Beale, *Science* **2021**, *371*, 1103–1104.

[2] a) F. Zhao, X. Zai, Z. Zhang, J. Xu, W. Chen, *NPJ Vaccines* **2022**, *7*, 167; b) W. T. Harvey, A. M. Carabelli, B. Jackson, R. K. Gupta, E. C. Thomson, E. M. Harrison, C. Ludden, R. Reeve, A. Rambaut, C.-G. U. Consortium, S. J. Peacock, D. L. Robertson, *Nat Rev Microbiol* **2021**, *19*, 409–424; c) S. S. Abdool Karim, T. de Oliveira, *N Engl J Med* **2021**, *384*, 1866–1868.

[3] P. A. Desingu, K. Nagarajan, *J Med Virol* **2022**, *94*, 5077–5079.

[4] a) A. Vitiello, F. Ferrara, A. M. Auti, M. Di Domenico, M. Boccellino, *J Intern Med* **2022**, *292*, 81–90; b) K. E. Lyke, R. L. Atmar, C. D. Islas, C. M. Posavad, D. Szydlo, R. Paul Chourdhury, M. E. Deming, A. Eaton, L. A. Jackson, A. R. Branche, H. M. El Sahly, C. A. Rostad, J. M. Martin, C. Johnston, R. E. Rupp, M. J. Mulligan, R. C. Brady, R. W. Frenck, Jr., M. Backer, A. C. Kottkamp, T. M. Babu, K. Rajakumar, S. Edupuganti, D. Dobrzynski, R. N. Coler, J. I. Archer, S. Crandon, J. A. Zemanek, E. R. Brown, K. M. Neuzil, D. S. Stephens, D. J. Post, S. U. Nayak, M. S. Suthar, P. C. Roberts, J. H. Beigel, D. C. Montefiori, D. S. Group, *Cell Rep Med* **2022**, *3*, 100679.

[5] a) P. Qu, J. P. Evans, J. N. Faraone, Y. M. Zheng, C. Carlin, M. Anghelina, P. Stevens, S. Fernandez, D. Jones, G. Lozanski, A. Panchal, L. J. Saif, E. M. Oltz, K. Xu, R. J. Gumina, S. L. Liu, *Cell Host Microbe* **2023**, *31*, 9–17 e3; b) X. L. Jiang, K. L. Zhu, X. J. Wang, G. L. Wang, Y. K. Li, X. J. He, W. K. Sun, P. X. Huang, J. Z. Zhang, H. X. Gao, E. H. Dai, M. J. Ma, *Lancet Infect Dis* **2023**, *23*, 28–30.

[6] R. K. Gupta, *Nat Rev Immunol* **2021**, *21*, 340–341.

[7] a) T. Zhang, R. Deng, Y. Wang, C. Wu, K. Zhang, C. Wang, N. Gong, R. Ledesma-Amaro, X. Teng, C. Yang, T. Xue, Y. Zhang, Y. Hu, Q. He, W. Li, J. Li, *Nat Biomed Eng* **2022**, *6*, 957–967; b) H. Zhang, Z. Wang, F. Wang, Y. Zhang, H. Wang, Y. Liu, *Anal Chem* **2020**, *92*, 5546–5553; c) F. Li, X. Mao, F. Li, M. Li, J. Shen, Z. Ge, C. Fan, X. Zuo, *J Am Chem Soc* **2020**, *142*, 9975–9981; d) J. Wang, C. Jiang, J. Jin, L. Huang, W. Yu, B. Su, J. Hu, *Angew Chem Int Ed* **2021**, *60*, 13042–13049.

[8] a) L. J. Carter, L. V. Garner, J. W. Smoot, Y. Li, Q. Zhou, C. J. Saveson, J. M. Sasso, A. C. Gregg, D. J. Soares, T. R. Beskid, S. R. Jervey, C. Liu, *ACS Cent Sci* **2020**, *6*, 591–605; b) Q. Wu, C. Suo, T. Brown, T. Wang, S. A. Teichmann, A. R. Bassett, *Science Advances* **2021**, *7*, eabe5054; c) J. A. Plante, B. M. Mitchell, K. S. Plante, K. Debbink, S. C. Weaver, V. D. Menachery, *Cell Host Microbe* **2021**, *29*, 508–515; d) C. M. Victoriano, M. E. Pask, N. A. Malofsky, A. Seegmiller, S. Simmons, J. E. Schmitz, F. R. Haselton, N. M. Adams, *Sci Rep* **2022**, *12*, 11756.

[9] a) C. Zhang, T. Zheng, H. Wang, W. Chen, X. Huang, J. Liang, L. Qiu, D. Han, W. Tan, *Anal Chem* **2021**, *93*, 3325–3330; b) J. Joung, A. Ladha, M. Saito, N.-G. Kim, A. E. Woolley, M. Segel, R. P. J. Barretto, A. Ranu, R. K. Macrae, G. Faure, E. I. Ioannidi, R. N. Krajeski, R. Bruneau, M.-L. W. Huang, X. G. Yu, J. Z. Li, B. D. Walker, D. T. Hung, A. L. Greninger, K. R. Jerome, J. S. Gootenberg, O. O. Abudayyeh, F. Zhang, *N Engl J Med* **2020**, *383*, 1492–1494; c) H. Lee, H. Lee, S. H. Hwang, W. Jeong, D. E. Kim, *Anal Chim Acta* **2022**, *1212*, 339909; d) Y. Deng, T. Zhou, Y. Peng, M. Wang, L. Xiang, Y. Zhang, J. Li, J. Yang, G. Li, *Anal Chem* **2023**, *95*, 3358–3362; e) T. Chaibun, J. Puenpa, T. Ngamdee, N. Boonapatcharoen, P. Athamanolap, A. P. O'Mullane, S. Vongpunsawad, Y. Poovorawan, S. Y. Lee, B. Lertanantawong, *Nat Commun* **2021**, *12*, 802.

[10] a) B. Casati, J. P. Verdi, A. Hempelmann, M. Kittel, A. G. Klaebisch, B. Meister, S. Welker, S. Asthana, S. Di Giorgio, P. Boskovic, K. H. Man, M. Schopp, P. A. Ginno, B. Radlwimmer, C. E. Stebbins, T. Miethke, F. N. Papavasiliou, R. Pecori, *Nat Commun* **2022**, *13*, 3308; b) O. O. Abudayyeh, J. S. Gootenberg, *Science* **2021**, *372*, 914–915; c) Y. Chen, S. Yang, S. Peng, W. Li, F. Wu, Q. Yao, F. Wang, X. Weng, X. Zhou, *Chem Sci* **2019**, *10*, 2975–2979.

[11] a) J. S. Gootenberg, O. O. Abudayyeh, J. W. Lee, P. Essletzbichler, A. J. Dy, J. Joung, V. Verdine, N. Donghia, N. M. Daringer, C. A. Freije, C. Myhrvold, R. P. Bhattacharyya, J. Livny, A. Regev, E. V. Koonin, D. T. Hung, P. C. Sabeti, J. J. Collins, F. Zhang, *Science* **2017**, *356*, 438–442; b) J. P. Broughton, X. Deng, G. Yu, C. L. Fasching, V. Servellita, J. Singh, X. Miao, J. A. Streithorst, A. Granados, A. Sotomayor-Gonzalez, K. Zorn, A. Gopez, E. Hsu, W. Gu, S. Miller, C. Y. Pan, H. Guevara, D. A. Wadford, J. S. Chen, C. Y. Chiu, *Nat Biotechnol* **2020**, *38*, 870–874; c) X. Ding, K. Yin, Z. Li, R. V. Lalla, E. Ballesteros, M. M. Sfeir, C. Liu, *Nat Commun* **2020**, *11*, 4711; d) J. Arizti-Sanz, A. Bradley, Y. B. Zhang, C. K. Boehm, C. A. Freije, M. E. Grunberg, T. F. Kosoko-Thoroddsen, N. L. Welch, P. P. Pillai, S. Mantena, G. Kim, J. N. Uwanibe, O. G. John, P. E. Eromon, G. Kocher, R. Gross, J. S. Lee, L. E. Hensley, B. L. MacInnis, J. Johnson, M. Springer, C. T. Happi, P. C. Sabeti, C. Myhrvold, *Nat Biomed Eng* **2022**, *6*, 932–943.

[12] a) J. Yang, Y. Song, X. Deng, J. A. Vanegas, Z. You, Y. Zhang, Z. Weng, L. Avery, K. D. Dieckhaus, A. Peddi, Y. Gao, Y. Zhang, X. Gao, *Nat Chem Biol* **2023**, *19*, 45–54; b) P. Fozouni, S. Son, M. Diaz de Leon Derby, G. J. Knott, C. N. Gray, M. V. D'Ambrosio, C. Zhao, N. A. Switz, G. R. Kumar, S. I. Stephens, D. Boehm, C. L. Tsou, J. Shu, A. Bhuiya, M. Armstrong, A. R. Harris, P. Y. Chen, J. M. Osterloh, A. Meyer-Franke, B. Joehnk, K. Walcott, A. Sil, C. Langelier, K. S. Pollard, E. D. Crawford, A. S. Puschnik, M. Phelps, A. Kistler, J. L. DeRisi, J. A. Doudna, D. A. Fletcher, M. Ott, *Cell* **2021**, *184*, 323–333 e329; c) H. Li, J. Yang, G. Wu, Z. Weng, Y. Song, Y. Zhang, J. A. Vanegas, L. Avery, Z. Gao, H. Sun, Y. Chen, K. D. Dieckhaus, X. Gao, Y. Zhang, *Angew Chem Int Ed* **2022**, *61*, e202203826. d) Y. Dai, R. A. Somoza, L. Wang, J. F. Welter, Y. Li, A. I. Caplan, C. C. Liu, *Angew Chem Int Ed* **2019**, *58*, 17399–17405; e) J. Zhang, H. Lv, L. Li, M. Chen, D. Gu, J. Wang, Y. Xu, *Front Microbiol* **2021**, *12*, 751408. f) A. Ghouneimy, M. Mahfouz, *Nat Biomed Eng* **2022**, *6*, 925–927.

[13] a) F. Hong, D. Ma, K. Wu, L. A. Mina, R. C. Luiten, Y. Liu, H. Yan, A. A. Green, *Cell* **2020**, *180*, 1018–1032 e1016; b) C. A. Freije, P. C. Sabeti, *Cell Host Microbe* **2021**, *29*, 689–703.

[14] C. B. F. Vogels, A. F. Brito, A. L. Wyllie, J. R. Fauver, I. M. Ott, C. C. Kalinich, M. E. Petrone, A. Casanovas-Massana, M. Catherine Muenker, A. J. Moore, J. Klein, P. Lu, A. Lu-Culligan, X. Jiang, D. J. Kim, E. Kudo,

10.1002/anie.202304298

T. Mao, M. Moriyama, J. E. Oh, A. Park, J. Silva, E. Song, T. Takahashi, M. Taura, M. Tokuyama, A. Venkataraman, O. E. Weizman, P. Wong, Y. Yang, N. R. Cheemarla, E. B. White, S. Lapidus, R. Earnest, B. Geng, P. Vijayakumar, C. Odio, J. Fournier, S. Bermejo, S. Farhadian, C. S. Dela Cruz, A. Iwasaki, A. I. Ko, M. L. Landry, E. F. Foxman, N. D. Grubaugh, *Nat Microbiol* **2020**, *5*, 1299–1305.

[15] a) H. Tegally, E. Wilkinson, M. Giovanetti, A. Iranzadeh, V. Fonseca, J. Giandhari, D. Doolabh, S. Pillay, E. J. San, N. Msomi, K. Mlisana, A. von Gottberg, S. Walaza, M. Allam, A. Ismail, T. Mohale, A. J. Glass, S. Engelbrecht, G. Van Zyl, W. Preiser, F. Petruccione, A. Sigal, D. Hardie, G. Marais, N. Y. Hsiao, S. Korsman, M. A. Davies, L. Tyers, I. Mudau, D. York, C. Maslo, D. Goedhals, S. Abrahams, O. Laguda-Akingba, A. Alisoltani-Dehkordi, A. Godzik, C. K. Wibmer, B. T. Sewell, J. Lourenco, L. C. J. Alcantara, S. L. Kosakovsky Pond, S. Weaver, D. Martin, R. J. Lessells, J. N. Bhiman, C. Williamson, T. de Oliveira, *Nature* **2021**, *592*, 438–443; b) N. G. Davies, C. I. Jarvis, C. C.-W. Group, W. J. Edmunds, N. P. Jewell, K. Diaz-Ordaz, R. H. Keogh, *Nature* **2021**, *593*, 270–274; c) N. G. Davies, S. Abbott, R. C. Barnard, C. I. Jarvis, A. J. Kucharski, J. D. Munday, C. A. B. Pearson, T. W. Russell, D. C. Tully, A. D. Washburne, T. Wenseleers, A. Gimma, W. Waites, K. L. M. Wong, K. van Zandvoort, J. D. Silverman, C. C.-W. Group, C.-G. U. Consortium, K. Diaz-Ordaz, R. Keogh, R. M. Eggo, S. Funk, M. Jit, K. E. Atkins, W. J. Edmunds, *Science* **2021**, *372*, eabg3055.

[16] a) A. Kruger, A. Burkle, K. Hauser, A. Mangerich, *Nat Commun* **2020**, *11*, 2174; b) Y. Hao, Y. Li, L. Song, Z. Deng, *J Am Chem Soc* **2021**, *143*, 3065–3069; c) J. Zhang, P. Zhao, W. Li, L. Ye, L. Li, Z. Li, M. Li, *Angew Chem Int Ed* **2022**, *61*, e202117562; d) Y. Yang, J. Wang, W. Huang, G. Wan, M. Xia, D. Chen, Y. Zhang, Y. Wang, F. Guo, J. Tan, H. Liang, B. Du, L. Yu, W. Tan, X. Duan, Q. Yuan, *Adv Mater* **2022**, *34*, e2203224.

[17] a) J. Shi, Y. Fang, *Adv Mater* **2019**, *31*, e1804895; b) X. Wang, M. Zhu, X. Li, Z. Qin, G. Lu, J. Zhao, Z. Zhang, *Adv Mater* **2022**, *34*, e2204066;

[18] a) A. S. Lauring, P. N. Malani, *JAMA* **2021**, *326*, 880; b) X. Huang, E. Kon, X. Han, X. Zhang, N. Kong, M. J. Mitchell, D. Peer, W. Tao, *Nat Nanotechnol* **2022**, *17*, 1027–1037.

[19] a) Y. Wang, A. Yan, D. Song, C. Dong, M. Rao, Y. Gao, R. Qi, X. Ma, Q. Wang, H. Xu, H. Liu, J. Han, M. Duan, S. Liu, X. Yu, M. Zong, J. Feng, J. Jiao, H. Zhang, M. Li, B. Yu, Y. Wang, F. Meng, X. Ni, Y. Li, Z. Shen, B. Sun, X. Shao, H. Zhao, Y. Zhao, R. Li, Y. Zhang, G. Du, J. Lu, C. You, H. Jiang, L. Zhang, L. Wang, C. Dou, Z. Liu, J. Zhao, *Cell Discov* **2023**, *9*, 3; b) P. Arora, A. Cossmann, S. R. Schulz, G. M. Ramos, M. V. Stankov, H.-M. Jäck, G. M. N. Behrens, S. Pöhlmann, M. Hoffmann, *The Lancet Infectious Diseases* **2023**, *23*, 147–148.

10.1002/anie.202304298

WILEY-VCH

RESEARCH ARTICLE

Entry for the Table of Contents

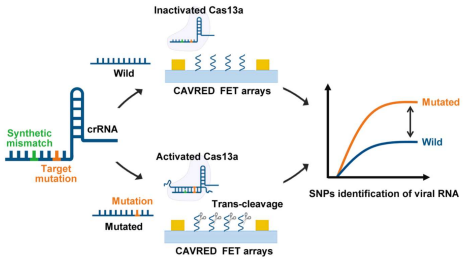

A CRISPR-based Amplification-free Viral RNA Electrical Detection platform (CAVRED) is reported for rapid and ultrasensitive detection and identification of SARS-CoV-2 and its variants. By combining CRISPR diagnostic technology with highly sensitive field-effect transistor arrays, CAVRED demonstrated RT-PCR-equivalent sensitivity without preamplification and achieved simultaneous profiling of 9 critical RNA mutations associated with SARS-CoV-2 variants of concern at single-nucleotide resolution. Owing to the advantages of high accuracy, sensitivity, and fast speed, CAVRED paves the way for rapid and large-scale epidemic screening.